New Full-Diversity Space-Time-Frequency Block Codes with Simplified Decoders for MIMO-OFDM Systems

Mostafa SHAHABINEJAD, Zahra MOHAMMADIAN, Siamak TALEBI

Department of Electrical Engineering, Shahid Bahonar University of Kerman, Pajohesh Square, Kerman, Iran

m.shahbinezhad@gmail.com, z.mohammadian87@gmail.com, siamak.talebi@uk.ac.ir

Abstract. *Multiple-input multiple-output orthogonal frequency-division multiplexing (MIMO-OFDM) is known as a promising solution for wideband wireless communications. This is why it has been considered as a powerful candidate for IEEE 802.11n standard. Numerous space-frequency block codes (SFBCs) and space-time-frequency block codes (STFBCs) have been proposed so far for implementing MIMO-OFDM systems. In this paper, at first we propose new full-diversity STFBCs with high coding gain in time-varying channels; the construct method for this structure is using orthogonal space-time block code for an arbitrary number of transmit antennas and then we propose a decoder with linear complexity for our proposed coding scheme. Simulation results verify that the proposed STFBCs outperform other recently published STFBCs.*

Keywords

Channel delay profile, fading channels, space-time-frequency coding, MIMO-OFDM systems.

1. Introduction

Wireless communication channels suffer from 2 undesired phenomena, namely fading and intersymbol interference (ISI). Space-time coding is one of the most advanced multiple-input multiple-output (MIMO) systems used to deal with flat fading channels [1-5]. High speed data transmission could turn the flat-fading channels into the frequency-selective ones, and this causes the intersymbol interference (ISI) effect, in addition to fading [6]. Space-time coding can be used in frequency-selective channels too [7], but in this case, equalizers are needed at the receiver that follows the complexity of the receiver and the loss of the frequency diversity. Indeed, in the frequency-selective channels, due to L different paths between each pair of transmit and receive antennas, there are L different replicas of each transmitted signal at the receiver. This multipath phenomenon seems to be distasteful at first, but it could be used as a source of diversity.

In order to deal with the ISI effect of the channel, orthogonal frequency-division multiplexing (OFDM) have been developed. OFDM spreads symbols over a larger time slot, using orthogonal subcarriers for modulating different symbols. In fact, OFDM transforms the wideband channels into a set of narrowband flat-fading sub-channels.

MIMO-OFDM systems take advantage of both MIMO and OFDM to tackle the fading and multipath effects, respectively. Space-frequency block codes (SFBCs) and space-time-frequency block codes (STFBCs) are 2 schemes for implementing MIMO-OFDM systems [6-19]. SFBCs use both the spatial and frequency diversities [8-11]. STFBCs utilize more than 1 timeslot by coding across multiple OFDM blocks. Design criteria of STFBCs are provided in [12, 13]. The added temporal dimension can be useful from 2 aspects: first, it can be used to reduce the receiver complexity of the STFBCs upon quasi-static channels [15, 16]. Second, it can be utilized as an additional diversity source when channel varies for different OFDM blocks [12,14,15]. When the channel behavior changes for different OFDM blocks, the maximum diversity advantage of the STFBCs is $M_t M_r L \times \mathrm{rank}(R_T)$, where R_T denotes the temporal correlation matrix of the channel [12]. To date, a lot of researches have been proposed to address tradeoff among code rate, performance of the code and decoding complexity of SFBCs and STFBCs. By using the existing space-time block codes (STBCs), primary SFBCs were designed by substituting time slots for the frequency subcarriers [7]. In [8] and [18] the authors have been designed rate-1 full-diversity SF codes with high coding gain. In [9], authors proposed a rate-2 SFBC for 2 transmit antennas and 2-ray frequency selective channels. Systematic construction of high-rate M_t symbol per channel use (s/cu) SFBCs are considered in [11] for M_t transmit antennas, but the proposed code provides a tradeoff between the code rate and the decoding complexity.

In [14], linear transform based full-diversity STFBCs and SFBCs are proposed which feature the best performance to the best of our knowledge. In [15], authors presented a new class of full-diversity STFBCs and SFBCs based on the generalized block-diagonal quasi-orthogonal

STBCs. An orthogonal rate-2/3 STFBC is proposed in [17] for 2 transmit antennas. In [10], we have proposed a systematic method to design full-diversity SFBCs for an arbitrary number of transmit antennas with high coding gain and moderate complexity decoding.

1.1 Main Contribution

The main contributions of this paper can be presented as follows:

1) We design a new class of STFBCs for an arbitrary number of transmit antennas. The codewords of new STFBCs are constructed by putting together a number of orthogonal space-time block codes (OSTBCs) in which a linear combination of symbols is embedded. In this new scheme for 2 transmit antennas we exert Alamouti code and for more transmit antennas we use the OSTBCs that are proposed in [2]. In this structure the rate of each STFBCs codeword is equal to the rate of the STBCs codeword used to construct it. The advantage of new codes is its high coding gain in compare with previously proposed codes. In the last, the simulation results confirm this claim.

2) We suggest a decoder with linear complexity for the designed codes. Specifically, by using the fact that neighboring subcarriers undergo similar fading, we decode linear combinations of symbols separately. Then, by applying the Hermitian of the precoder matrix to the decoded data, symbols are detected. We believe that our proposed decoding method can perform properly regarding its simple structure.

1.2 Organization

The rest of the paper is organized as follows. In the following section, we present the mathematical model of the space-time-frequency coded MIMO-OFDM systems. In Section 3, we unfold details of the newly proposed STFBCs. In Section 4, we discuss how the simplified decoder could be employed for our coding scheme. Section 5 holds simulation results. In the last section, conclusion of the paper is presented.

Notations: In this article matrices are shown with capital boldface letters and vectors with boldface letters. Superscripts $(.)^T$, $(.)^\dagger$ and $(.)^*$ specify transpose, Hermitian and complex conjugation, respectively. $\circ$, and $\otimes$ are used for the Hadamard and the tensor products, respectively. Notation $diag(a_1, a_2, \dots, a_n)$ denotes a diagonal $n \times n$ matrix whose diagonal entries are $a_1, a_2, \dots, a_n$, and $\boldsymbol{V}(t_1, t_2, \dots, t_n)$ is a Vandermonde matrix as below:

$$\boldsymbol{V}(t_1, t_2, \dots, t_n) = \begin{bmatrix} 1 & 1 & \cdots & 1 \\ t_1 & t_2 & \cdots & t_n \\ \vdots & \vdots & \ddots & \vdots \\ t_1^{n-1} & t_2^{n-1} & \cdots & t_n^{n-1} \end{bmatrix} \in \mathbb{C}^{n \times n}.$$

$j = \sqrt{-1}$, $\lfloor \cdot \rfloor$and $\|\cdot\|_F$ stand for the floor operation and Frobenius norm, respectively; $\mathbf{1}_a$ is a matrix of size $a \times a$ whose all entries are equal to 1, and $\boldsymbol{I}_a$ represents an identity matrix of size $a \times a$.

2. System Model

In this section, we describe the system model of a MIMO-OFDM system. Consider a space-time-frequency coded MIMO-OFDM system with M_t transmit antennas, M_r receive antennas, and N subcarriers with K successive OFDM blocks. We assume that between each pair of transmit and receive antenna there are L independent delay paths with the same delay and power profiles (DPPs). Channel impulse response during the k^{th} OFDM block from the transmit antenna i to the receive antenna j is given by [12]:

$$h_{i,j}^k(\zeta) = \sum_{l=0}^{L-1} \alpha_{i,j}^k(l)\delta(\zeta - \zeta_l), \; k = 1, 2, \dots, K \quad (1)$$

where ζ_l's are delays and $\alpha_{i,j}^k(l)$'s are zero-mean complex Gaussian random variables, indicating the complex amplitude for the l^{th} path of the i^{th} transmit and the j^{th} receive antennas in the k^{th} OFDM block. The power of the L^{th} path is equal to $E\left|\alpha_{i,j}^k(l)\right|^2 = \delta_l^2$, where E stands for the expectation.

Each codeword of a STFBC can be formed as a $KN \times M_t$ matrix as below:

$$\boldsymbol{C} = [\boldsymbol{C}_1^T \quad \boldsymbol{C}_2^T \quad \cdots \quad \boldsymbol{C}_K^T]^T \quad (2)$$

where

$$\boldsymbol{C}_k = \begin{bmatrix} c_1^k(0) & c_2^k(0) & \dots & c_{M_t}^k(0) \\ c_1^k(1) & c_2^k(1) & \dots & c_{M_t}^k(1) \\ \vdots & \vdots & \ddots & \vdots \\ c_1^k(N-1) & c_2^k(N-1) & \dots & c_{M_t}^k(N-1) \end{bmatrix},$$

$$k = 1,2, \dots, K. \quad (3)$$

In (3), $c_i^k(n)$'s are symbols or linear combinations of them which are transmitted over the n^{th} subcarrier by the transmit antenna $i$and the k^{th} OFDM block. After applying an N-point inverse fast Fourier transform to each column of $\boldsymbol{C}_k$ and adding cyclic prefix, the i^{th} column of $\boldsymbol{C}_k$ is transmitted by the transmit antenna i.

The received signal at the j^{th} receive antenna and the k^{th} OFDM block, after crossing from matched filter, removing cyclic prefix, and performing fast Fourier transform is given as:

$$r_j^k(n) = \sum_{i=1}^{M_t} c_i^k(n) H_{i,j}^k(n) + \mathcal{N}_j^k(n),$$

$$n = 0,1, \dots, N-1 \quad (4)$$

where $\mathcal{N}_j^k(n)$ denotes the zero-mean additive white complex Gaussian noise corresponding to the n^{th} frequency subcarrier,

$$H_{i,j}^{k}(n) = \sum_{l=0}^{L-1} \alpha_{i,j}^{k}(l) w^{n\zeta_l} \tag{5}$$

represents the channel frequency response at the n^{th} subcarrier between the transmit antenna i and the receive antenna j, and $w = e^{-j2\pi\frac{BW}{N}}$, where BW is the total bandwidth of the system.

3. Newly Proposed STFBCs for MIMO-OFDM Systems

3.1 Structure of the Proposed STFBCs:

The initial structure of the proposed STFBC could be considered as below:

$$\boldsymbol{C}_k = [\boldsymbol{G}_{k,1}^T, \boldsymbol{G}_{k,2}^T, \dots, \boldsymbol{G}_{k,P}^T, \boldsymbol{Z}^T]^T \in \mathbb{C}^{N\times M_t},$$
$$k = 1, 2, \dots, K \tag{6}$$

where $P = \left\lfloor \frac{N}{\Gamma \mathrm{L}} \right\rfloor$, $\boldsymbol{G}_{k,p}$'s for $p = 1,2,\dots,P$ are matrices of size $\Gamma L \times M_t$ whose constructions are mutually exclusive, and Γ denotes the number of time slots used to generate the OSTBCs, and $\boldsymbol{Z}$ is an $(N - P\Gamma L) \times M_t$ matrix of zeros.

First, taking the data symbol vector $[s_1^p, s_2^p, \dots, s_{\mathrm{L}KM_t}^p]^T$ from a constellation such as BPSK or QPSK, the precoded vector $[x_1^p, x_2^p, \dots, x_{\mathrm{L}KM_t}^p]^T$ could be derived from equation below:

$$\left[x_1^p, x_2^p, \dots, x_{\mathrm{L}KM_t}^p\right]^T = \boldsymbol{V}[s_1^p, s_2^p, \dots, s_{\mathrm{L}KM_t}^p]^T \in \mathbb{C}^{K\mathrm{L}M_t\times 1} \tag{7}$$

where $\boldsymbol{V}$ is a Vandermonde matrix of size $KLM_t \times KLM_t$ with the same parameters as those of (43) in [12]. Then, $\boldsymbol{G}_{k,p}$'s are generated as:

$$\boldsymbol{G}_{k,p} = \begin{bmatrix} \boldsymbol{X}_{(k-1)\mathrm{L}+1}^p \\ \boldsymbol{X}_{(k-1)\mathrm{L}+2}^p \\ \vdots \\ \boldsymbol{X}_{k\mathrm{L}}^p \end{bmatrix} \in \mathbb{C}^{\Gamma L\times M_t}, k = 1,2,\dots,K. \tag{8}$$

In (8), each $\boldsymbol{X}_l^p \in \mathbb{C}^{\Gamma\times M_t}$ denote an OSTBC including M_t distinct x_i^p's, and Γ is the number of time slots in each OSTBC.

In the following, we enhance the coding advantage of the proposed STFBCs by adding a new parameter, namely γ_{SD}, to its design in order to attain a better performance. The structure of $\boldsymbol{C}_k$when the parameter γ_{SD} is added to the code design changes to $\boldsymbol{C}_k^M$by the following equation:

$$\boldsymbol{C}_k^M = \boldsymbol{P}\boldsymbol{C}_k, \quad k = 1, 2, \dots, K \tag{9}$$

where $\boldsymbol{P} = \operatorname{diag}(\boldsymbol{P}_t, \boldsymbol{Z}_b) \in \mathbb{N}^{N\times N}$, and

$$\boldsymbol{P}_t = \operatorname{diag}\left(\overbrace{\boldsymbol{P}_b, \boldsymbol{P}_b, \dots, \boldsymbol{P}_b}^{\text{Number of} \boldsymbol{P}_b\text{'s}= \left\lfloor \frac{N}{\mathrm{L}\gamma_{SD}} \right\rfloor}, \boldsymbol{P}_b' \right) \otimes$$

$$\boldsymbol{I}_\Gamma \in \mathbb{C}^{\mathrm{L}\gamma_{SD}\left\lfloor \frac{N}{\mathrm{L}\gamma_{SD}} \right\rfloor \times \mathrm{L}\gamma_{SD}\left\lfloor \frac{N}{\mathrm{L}\gamma_{SD}} \right\rfloor} \tag{10}$$

In (10),

$$\boldsymbol{P}_b = [\boldsymbol{P}_1^T \quad \boldsymbol{P}_2^T \quad \dots \quad \boldsymbol{P}_\mathrm{L}^T]^{\boldsymbol{T}} \in \mathbb{N}^{\mathrm{L}\frac{\gamma_{SD}}{\Gamma}\times \mathrm{L}\frac{\gamma_{SD}}{\Gamma}} \tag{11}$$

where

$$\boldsymbol{P}_i = \left[\boldsymbol{e}_i^T \quad \boldsymbol{e}_{\mathrm{L}+i}^T \quad \dots \quad \boldsymbol{e}_{\left(\frac{\gamma_{SD}}{\Gamma}-1\right)\mathrm{L}+i}^T\right]^{\boldsymbol{T}} \in \mathbb{N}^{\frac{\gamma_{SD}}{\Gamma}\times \mathrm{L}\frac{\gamma_{SD}}{\Gamma}},$$
$$i = 1, 2, \dots, \mathrm{L}. \tag{12}$$

In (12), $\boldsymbol{e}_i \in \mathbb{C}^{1\times \mathrm{L}\frac{\gamma_{SD}}{\Gamma}}$ is a vector whose components are all zeros except for the i^{th} element that is 1, and

$$\boldsymbol{P}_b' = [\boldsymbol{P}_1'^T \quad \boldsymbol{P}_2'^T \quad \dots \quad \boldsymbol{P}_{\left\lfloor\frac{\gamma_r}{\mathrm{L}\Gamma}\right\rfloor}'^T]^T \in \mathbb{C}^{\mathrm{L}\left\lfloor\frac{\gamma_r}{\mathrm{L}\Gamma}\right\rfloor\times \mathrm{L}\left\lfloor\frac{\gamma_r}{\mathrm{L}\Gamma}\right\rfloor} \tag{13}$$

where $\gamma_r = N - \mathrm{L}\gamma_{SD}\left\lfloor \frac{N}{\mathrm{L}\gamma_{SD}} \right\rfloor$ and

$$\boldsymbol{P}'_i = \left(\boldsymbol{e}'^T_i \quad \boldsymbol{e}'^T_{\left\lfloor\frac{\gamma_r}{\mathrm{L}\Gamma}\right\rfloor+i} \quad \dots \quad \boldsymbol{e}'^T_{(\mathrm{L}-1)\left\lfloor\frac{\gamma_r}{\mathrm{L}\Gamma}\right\rfloor+i}\right)^T \in \mathbb{C}^{\mathrm{L}\times \mathrm{L}\left\lfloor\frac{\gamma_r}{\mathrm{L}\Gamma}\right\rfloor},$$
$$i = 1,2,\dots,\left\lfloor\frac{\gamma_r}{\mathrm{L}\Gamma}\right\rfloor. \tag{14}$$

In (14), the entries of $\boldsymbol{e}'_i \in \mathbb{C}^{1\times\left\lfloor\frac{\gamma_r}{\mathrm{L}\Gamma}\right\rfloor}$ are zero except for the i^{th} element that is 1. And $\boldsymbol{Z}_b$ is a $(\gamma_r - \mathrm{L}\Gamma\left\lfloor\frac{\gamma_r}{\mathrm{L}\Gamma}\right\rfloor) \times (\gamma_r - \mathrm{L}\Gamma\left\lfloor\frac{\gamma_r}{\mathrm{L}\Gamma}\right\rfloor)$ matrix of zeros. In order to construct our STFBCs for arbitrary numbers of transmit antennas, we can readily utilize an OSTBC, which is designed for M_t transmit antennas.

The receiver complexity of the proposed STFBCs is in the order of (M^{KLM_t}) for the ML decoder, where $M$is the constellation size. In Section 4, we propose a simplified decoder for our proposed codes.

3.2 Permutation Parameter ($\boldsymbol{\gamma_{SD}}$)

During the code design process, parameter γ_{SD} is embedded in the structure of code so that proposed codes have the maximum coding advantage.

According to the performance criteria in [12], for maximizing the coding advantage of a STFBC, we should maximize the minimum determinant of Ξ over all pairs of distinct codewords $\boldsymbol{C}$ and $\widehat{\boldsymbol{C}}$, where

$$\Xi \triangleq \Delta \circ \boldsymbol{R} \in \mathbb{C}^{KN\times KN}. \tag{15}$$

In (15), $\Delta \triangleq (\boldsymbol{C} - \widehat{\boldsymbol{C}})(\boldsymbol{C} - \widehat{\boldsymbol{C}})^\dagger$ and $\boldsymbol{R} \triangleq \boldsymbol{R}_T \otimes \boldsymbol{R}_F$, where $\boldsymbol{R}_F$ and $\boldsymbol{R}_T$ are the frequency and temporal correlation matrices, respectively [12]. In order to maximize the coding advantage of our codes, for the sake of simplicity, we suppose that 2 distinct codewords $\boldsymbol{C}$ and $\widehat{\boldsymbol{C}}$ are dissimilar only in symbol s_1. With this assumption we can confirm that maximum coding advantage of our proposed code presented in (9), consequences of maximizing the determinant of the following matrix:

$$\widehat{\boldsymbol{\Xi}} = (\boldsymbol{1}_{LK} \otimes \boldsymbol{I}_2) \circ (\boldsymbol{R}_T \otimes \boldsymbol{R}_F). \tag{16}$$

In (16), $\boldsymbol{R}_F = \boldsymbol{W}\mathrm{diag}(\sigma_0^2, \sigma_1^2, \dots, \sigma_{L-1}^2)\boldsymbol{W}^\dagger$ and $\boldsymbol{W} \in \mathbb{C}^{2L\times L}$ is defined as follows:

$$\boldsymbol{W} = \begin{bmatrix} 1 & 1 & \cdots & 1 \\ w^{\zeta_0} & w^{\zeta_1} & \cdots & w^{\zeta_{L-1}} \\ w^{(\gamma_{SD}+1)\zeta_0} & w^{(\gamma_{SD}+1)\zeta_1} & \cdots & w^{(\gamma_{SD}+1)\zeta_{L-1}} \\ w^{(\gamma_{SD}+2)\zeta_0} & w^{(\gamma_{SD}+2)\zeta_1} & \cdots & w^{(\gamma_{SD}+2)\zeta_{L-1}} \\ \vdots & \vdots & \cdots & \vdots \\ w^{((L-1)\gamma_{SD}+1)\zeta_0} & w^{((L-1)\gamma_{SD}+1)\zeta_1} & \cdots & w^{((L-1)\gamma_{SD}+1)\zeta_{L-1}} \\ w^{((L-1)\gamma_{SD}+2)\zeta_0} & w^{((L-1)\gamma_{SD}+2)\zeta_1} & \cdots & w^{((L-1)\gamma_{SD}+2)\zeta_{L-1}} \end{bmatrix} \quad (17)$$

and $\boldsymbol{R}_T$ is the temporal correlation matrix of the size $K \times K$. The element associated with the k^{th} row and the p^{th}column of $\boldsymbol{R}_T$ is obtained by $R_T(k,p) = v(k-p)$ where $v(k-p) = E\{\alpha_{i,j}^k(l)\alpha_{i,j}^p(l)^*\}$ [12].

Regarding (16) and (17) the coding advantage depends on γ_{SD}. When DPPs are available at the transmitter side, we verify γ_{SD} so as the proposed STFBCs have the maximum coding advantage and when DPPs are not available at the transmitter side, we exert the using interleave method in [14].

4. A Simplified Decoder for the Proposed Coding Scheme

4.1 Methodology

In this subsection, we present a new method which ultimately leads to a linear decoding process for our proposed coding scheme. It is worth mentioning that the receiver complexity of our proposed STFBCs is in the order of $O(M^{KLM_t})$ for the optimum ML decoder. Needless to say, this degree of complexity causes the rapid loss of energy at the receiver, which is undesirable. In comparison, as will be seen below, the simplified decoder leads to a very fast decoding process at the decoder.

Now, let us explore how the decoding method works. For the sake of simplicity and the clarity of exposition, let the number of time slots and receive antennas be 1, i.e., $K = M_R = 1$. Regarding (4), after applying the permutation parameter γ_{SD} to the code, the received signal associated with the $\boldsymbol{G}_{1,p}$ shown in (8) could be considered as follows (note that $K = 1$):

$$\boldsymbol{r}(l,p) = \sum_{i=1}^{M_t}\left(\boldsymbol{x}_{l_i}^p \circ \boldsymbol{h}_i(l,p)\right) + \boldsymbol{\mathcal{N}}(l,p),\ l = 1,2,\dots,L \quad (18)$$

where $\boldsymbol{x}_{l_i}^p \in \mathbb{C}^{\Gamma\times 1}$denotes the i^{th} column of $\boldsymbol{X}_l^p$,

$$\boldsymbol{h}_i(l,p) = \begin{bmatrix} H_{i,1}^1\left((l-1)\gamma_{SD} + (p-1)\Gamma\right) \\ H_{i,1}^1\left((l-1)\gamma_{SD} + 1 + (p-1)\Gamma\right) \\ \vdots \\ H_{i,1}^1\left((l-1)\gamma_{SD} + (\Gamma-1) + (p-1)\Gamma\right) \end{bmatrix} \in \mathbb{C}^{\Gamma\times 1},$$

$$\boldsymbol{\mathcal{N}}(l,p) = \begin{bmatrix} \mathcal{N}_1^1\left((l-1)\gamma_{SD} + (p-1)\Gamma\right) \\ \mathcal{N}_1^1\left((l-1)\gamma_{SD} + 1 + (p-1)\Gamma\right) \\ \vdots \\ \mathcal{N}_1^1\left((l-1)\gamma_{SD} + (\Gamma-1) + (p-1)\Gamma\right) \end{bmatrix} \in \mathbb{C}^{\Gamma\times 1},$$

and

$$\mathbf{r}(l,p) = \begin{bmatrix} \mathrm{r}_1^1\left((l-1)\gamma_{SD} + (p-1)\Gamma\right) \\ \mathrm{r}_1^1\left((l-1)\gamma_{SD} + 1 + (p-1)\Gamma\right) \\ \vdots \\ \mathrm{r}_1^1\left((l-1)\gamma_{SD} + (\Gamma-1) + (p-1)\Gamma\right) \end{bmatrix} \in \mathbb{C}^{\Gamma\times 1}.$$

Now, based on the fact that adjacent frequency subcarriers undergo similar fading, let us replace all elements of $\boldsymbol{h}_i(l,p)$ by the value of $\overline{h_i}(l,p) = \frac{1}{\Gamma}\sum_{\gamma=0}^{\Gamma-1} H_{i,1}^1((l-1)\gamma_{SD} + \gamma + (p-1)\Gamma)$. In doing this, one may easily rewrite (18) as follows:

$$\boldsymbol{r}(l,p) = \boldsymbol{X}_l^p\overline{\boldsymbol{h}}(l,p) + \boldsymbol{\mathcal{N}}(l,p) \in \mathbb{C}^{\Gamma\times 1},\quad l = 1,2,\dots,L \quad (19)$$

where $\overline{\boldsymbol{h}}(l,p) = [\overline{h_1}(l,p), \overline{h_2}(l,p), \dots, \overline{h_{M_t}}(l,p)]^T \in \mathbb{C}^{M_t\times 1}$. Interestingly, the obtained equation in (19) has the same structure as the system model of typical space-time coded MIMO systems. Hence, since that $\boldsymbol{X}_l^p$'s are OSTBCs, one can linearly decode the linear combinations of symbols involved in each $\boldsymbol{X}_l^p$, i.e.,$x_{(l-1)M_t+1}^p$ to $x_{lM_t}^p$ for $l = 1,2,\dots,L$. In the last step of the decoding operations, we obtain estimations of the transmitted symbols $\{s_1^p, s_2^p, \dots, s_{2L}^p\}$, say $\{\hat{s}_1^p, \hat{s}_2^p, \dots, \hat{s}_{2L}^p\}$, by the following equation:

$$\left[\hat{s}_1^p,\ \hat{s}_2^p, \dots, \hat{s}_{2L}^p\right]^{\mathrm{T}} = \boldsymbol{V}^H[\hat{x}_1^p, \hat{x}_2^p, \dots, \hat{x}_{2L}^p]^{\mathrm{T}} \quad (20)$$

where $\hat{x}_1^{\mathrm{p}}, \hat{x}_2^{\mathrm{p}}, \dots, \hat{x}_{2L}^{\mathrm{p}}$ are estimations of $x_1^{\mathrm{p}}, x_2^{\mathrm{p}}, \dots, x_{2L}^{\mathrm{p}}$, respectively. It is notable that since the precoder matrix $\boldsymbol{V}$ is a unitary matrix, it does not change the norm of the additive noise.

Although we have only explained the decoding method for the proposed SFBCs ($K = 1$) and 1 receive antenna ($M_r = 1$), it is just as straightforward to demonstrate that the proposed simplified decoding solution could be easily extended to include the proposed STFBCs ($K > 1$) and any arbitrary number of the receive antennas. It is important to point out that with the proposed decoding method, we are only dealing with a linear decoding process, and thus the decoder is relatively free of the complexity of the order of $O(M^{LM_t})$ and $O(M^{LM_tK})$ associated with the ML decoder of the proposed SFBCs and STFBCs, respectively. In the following subsection, we discuss how the simplified decoder performs for different situations.

4.2 Performance Evaluation of the Proposed Simplified Decoder

Our proposed decoder is a suboptimum one due to 2 reasons: first, we use the average value of the frequency fading coefficients rather than their original values. This, i.e., replacing adjacent fading coefficients, can affect the performance especially when Γ increases. Second, we decode each bunch of M_t-fold x_i^p's separately, and then obtain $\hat{s}_i^p$'s using (20).Considering the following scenario, in which all $\hat{s}_i^p$'s are jointly decoded:

$$\min_{\hat{s}_1^p,\hat{s}_2^p,\ldots,\hat{s}_{LM_t}^p} \left\| \boldsymbol{r}(l,p) - \boldsymbol{X}_l^p \overline{\boldsymbol{h}}(l,p) \right\|_F , \tag{21}$$

decoding x_i^p's separately can affect the performance of the simplified decoder especially when L and/or K increase. The following example seems to be beneficial to support our statements.

Example: Suppose that $\Gamma = L = M_t = 2$. At the transmitter we combine each $LM_t = 4$ symbols together. For the first LM_t symbols we have:

$$[x_1, x_2, x_3, x_4]^T = V_4[s_1, s_2, s_3, s_4]^T, \tag{22}$$

then the combinations of symbols are located at $\boldsymbol{G}_{1,1}$ as below:

$$\boldsymbol{G}_{1,1} = \begin{bmatrix} \boldsymbol{X}_1^1 \\ \boldsymbol{X}_2^1 \end{bmatrix} \tag{23}$$

where

$$X_1^1 = \begin{bmatrix} x_1 & x_2 \\ -x_2^* & x_1^* \end{bmatrix}, X_2^1 = \begin{bmatrix} x_3 & x_4 \\ -x_4^* & x_3^* \end{bmatrix}.$$

In order to simplify the decoder, we consider the average value of the frequency fading coefficients instead of their original values. Doing this, we have:

$$\begin{bmatrix} r_1^1(0) \\ r_1^1(1) \end{bmatrix} = \begin{bmatrix} x_1 \\ -x_2^* \end{bmatrix} \circ \begin{bmatrix} \bar{h}_1(1,1) \\ \bar{h}_1(1,1) \end{bmatrix} + \begin{bmatrix} x_2 \\ x_1^* \end{bmatrix} \circ \begin{bmatrix} \bar{h}_2(1,1) \\ \bar{h}_2(1,1) \end{bmatrix} + \begin{bmatrix} N_1^1(0) \\ N_1^1(1) \end{bmatrix} \tag{24}$$

instead of

$$\begin{bmatrix} r_1^1(0) \\ r_1^1(1) \end{bmatrix} = \begin{bmatrix} x_1 \\ -x_2^* \end{bmatrix} \circ \begin{bmatrix} H_{1,1}^1(0) \\ H_{1,1}^1(1) \end{bmatrix} + \begin{bmatrix} x_2 \\ x_1^* \end{bmatrix} \circ \begin{bmatrix} H_{2,1}^1(0) \\ H_{2,1}^1(1) \end{bmatrix} + \begin{bmatrix} N_1^1(0) \\ N_1^1(1) \end{bmatrix} \tag{25}$$

where in (24),

$$\bar{h}_1(1,1) = \tfrac{1}{2}\left(H_{1,1}^1(0) + H_{1,1}^1(1)\right),$$

$$\bar{h}_2(1,1) = \tfrac{1}{2}\left(H_{2,1}^1(0) + H_{2,1}^1(1)\right).$$

So, (24) can be written as:

$$\begin{bmatrix} r_1^1(0) \\ r_1^1(1) \end{bmatrix} = \begin{bmatrix} x_1 & x_2 \\ -x_2^* & x_1^* \end{bmatrix} \begin{bmatrix} \bar{h}_1(1,1) \\ \bar{h}_2(1,1) \end{bmatrix} + \begin{bmatrix} N_1^1(0) \\ N_1^1(1) \end{bmatrix}. \tag{26}$$

Hence (26) has the same structure as the system model of typical space-time coded MIMO systems. Now according to the structure of the code, which is constructed by using orthogonal codes, we can decode x_1 and x_2 linearly such as Alamouti STBC (in general OSTBCs) as below:

$$\hat{x}_1 = x_1 + \frac{N_1^1(0)}{\left|\bar{h}_1(1,1)\right|^2 + \left|\bar{h}_2(1,1)\right|^2},$$

$$\hat{x}_2 = x_2 + \frac{N_1^1(1)}{\left|\bar{h}_1(1,1)\right|^2 + \left|\bar{h}_2(1,1)\right|^2}.$$

Similarly, x_3 and x_4 are decoded. Also since the Vandermonde matrix is a unitary matrix ($\boldsymbol{V}\boldsymbol{V}^{\mathrm{H}} = \mathrm{I}$), by applying the Hermitian of the Vandermonde matrix to the decoded data, symbols are detected:

$$[\hat{s}_1, \hat{s}_2, \hat{s}_3, \hat{s}_4]^T = V_4^H[\hat{x}_1, \hat{x}_2, \hat{x}_3, \hat{x}_4]^T. \tag{27}$$

In the general case, the ML decoding associated with $\boldsymbol{G}_{k,p}$ is done as the equation at the bottom of the page. The sub-optimum decoder, on the other hand, results in

$$\hat{x}_{2l-1}^p = x_{2l-1}^p + \frac{N_1'(l,p)}{\left|\overline{h_1}(l,p)\right|^2 + \left|\overline{h_2}(l,p)\right|^2} \tag{28}$$

and

$$\hat{x}_{2l}^p = x_{2l}^p + \frac{N_2'(l,p)}{\left|\overline{h_1}(l,p)\right|^2 + \left|\overline{h_2}(l,p)\right|^2} \tag{29}$$

for $l = \{1, 2\}$ and $N_q'(l,p)$'s are noise terms.

$$\min_{s_1^p,s_2^p,s_3^p,s_4^p} \sum_{l=1}^{2} \left\| \begin{bmatrix} \mathrm{r}_1^1\left((l-1)\gamma_{SD} + 2p - 2\right) \\ \mathrm{r}_1^1\left((l-1)\gamma_{SD} + 2p - 1\right) \end{bmatrix} - \begin{bmatrix} x_{2l-1}^p \\ -x_{2l}^{p\,*} \end{bmatrix} \circ \begin{bmatrix} \mathrm{H}_{1,1}^1\left((l-1)\gamma_{SD} + 2p - 2\right) \\ \mathrm{H}_{1,1}^1\left((l-1)\gamma_{SD} + 2p - 1\right) \end{bmatrix} - \begin{bmatrix} x_{2l}^p \\ x_{2l-1}^{p\,*} \end{bmatrix} \circ \begin{bmatrix} \mathrm{H}_{2,1}^1\left((l-1)\gamma_{SD} + 2p - 2\right) \\ \mathrm{H}_{2,1}^1\left((l-1)\gamma_{SD} + 2p - 1\right) \end{bmatrix} \right\|_F$$

In the proposed simplified decoder, (28) and (29) show that only 2 (and in the general case, M_t) fading coefficients collaborate in the decoding process of the transmitted symbols separately. While in the ML decoding method, all LM_t fading coefficients cooperate to decode the transmitted data simultaneously.

5. Simulation Results

This section includes the simulation results, in which we compare the performance of our proposed STFBCs with those introduced in [14].In the simulations, we considered a MIMO-OFDM system with BW = 1 MHz and the length of cyclic prefix of 20 µs. We evaluated the performance of the new scheme by sketching average bit-error-rate (BER) versus average signal-to-noise-ratio (SNR). We compared the performance of the proposed codes against those of the BCDD codes and optimum STFBCs, presented in [14] for the unknown and the known DPPs cases, respectively. These codes are the best STFBCs in the literature to the best of authors' knowledge.

Note that the simplified decoder has the *linear complexity* for the proposed STFBCs, while the ML decoder leads to a complexity in the order of $\mathcal{O}(M^{LM_tK})$ for both the proposed and the coding scheme in [14].

Supposing that DPPs are unknown to the transmitter, a 2-ray equal power channel model with delay profile {0, 5} µs is considered in Fig. 1. In order to achieve a code rate equal to 1 Bit/s/Hz and to transfer bits to symbols, BPSK constellation is utilized for both the proposed and BCDD STFBCs. We furthermore assume that $K = 2$, N = 128, M_t = 2, and M_r = 1. Fig. 1 shows that our proposed STFBC outperforms the BCDD STFBCs in [14] when the ML decoder is utilized. Simulation results presented in Fig. 1 also depict that the performance of the proposed STFBC degrades when the simplified decoder is used. However, especially for high SNRs, the utilization of the proposed simplified decoder could still be of interest because it leads to a much faster decoding process than the ML decoder.

The same parameters of the system and channel, as those of Fig. 1, are considered in Fig. 2, except for M_r, which is set to 2. Regarding the BER values, our proposed STFBC outperforms the BCDD STFBC. For example, Fig. 2 shows that our proposed STFBC outdoes the BCDD code by almost 0.75 dB at BER = 10^{-6}. Simulation results associated with the simplified decoder are also presented in this case.

In the known DPPs case, a 2-ray equal power channel model with delay profile {0, 1} µs is considered. Fig. 3 demonstrates that our proposed optimized STFBC outperforms the optimum STFBC in [14]. For example, at BER = 10^{-4}, the proposed code achieves about 3 dB gain over the optimum STFBC in [14]. The other interesting point about the simulation results presented in Fig. 3 is that the proposed STFBC with the simplified linear decoder has the same performance as the optimum STFBC in [14] with the complexity in the order of $\mathcal{O}(M^8)$.

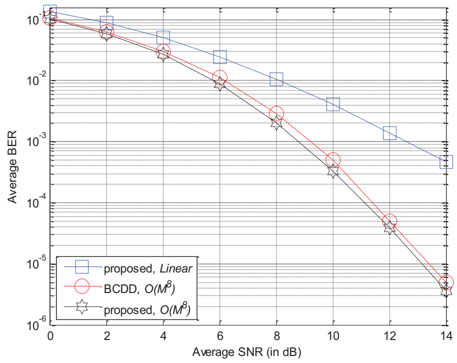

Fig. 1. BER performance for the 2-ray equal power frequency-selective channel with 5 µs delay spread, BPSK constellation, N = 128, $K = 2$, M_t = 2, M_r = 1, γ_{SD} = γ_{dpi} = 8, 1 bit/s/Hz.

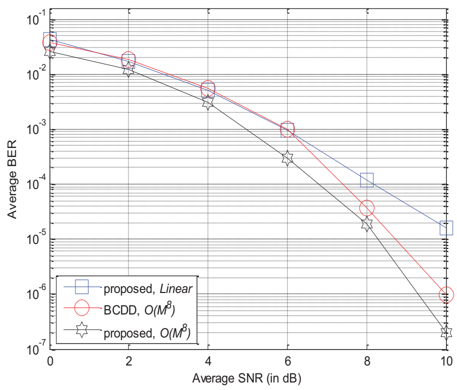

Fig. 2. BER performance for the 2-ray equal power frequency-selective channel with 5 µs delay spread, BPSK constellation, N=128, $K = 2$, M_t=2, M_r=2, γ_{SD}=γ_{dpi}= 8, 1 bit/s/Hz.

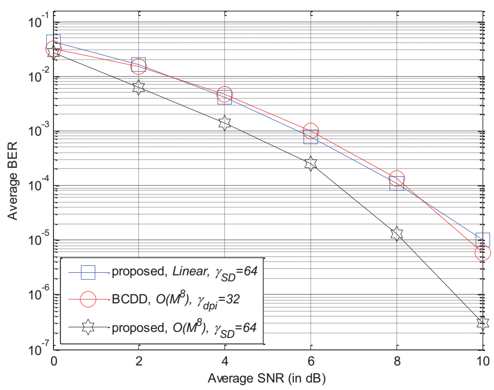

Fig. 3. BER performance for the 2-ray equal power frequency-selective channel with 1 μs delay spread, BPSK constellation, $K = 2$, N = 128, M_t = 2,M_r = 2, 1 bit/s/Hz.

As can be noticed from the simulation results presented in Figs. 1 to 3, the simplified linear decoder does not perform properly compared to the ML decoder for our proposed STFBCs. Now, based on the explanations provided in Section 4, let us present some simulation results which result in a more acceptable performance for the simplified decoder. To do this, we consider 2-ray equal power channels and SFBCs with 2, 3, and 4 transmit antennas respectively in Figs. 4, 5, and 6 (in all cases, M_r = 1).

In the simulations shown in Fig. 4, we set N = 1024, and consider a channel with 5 µs delay spread. Results show that our proposed code outperforms the BCDD SFBC, e.g., by nearly 0.5 dB at BER = 10^{-4}, and the simplified linear decoder performs satisfactorily especially at SNR slower than 16 dB.

Considering 3 transmit antennas, the symbol transmission rates are equal to 3/4 and 1 in our proposed code and the BCDD code, respectively. Hence, 16-QAM and 8-QAM constellations are used correspondingly for our proposed code and the BCDD code in order to attain the same bit transmission rate of 3 bits/s/Hz. In order to decode the received data, the sphere decoder is used for both codes. As results presented in Fig. 5 depict, our proposed code leads to better performance in comparison with the BCDD code. And, interestingly, the proposed simplified decoder outperforms the suboptimum sphere decoder. For example, as Fig. 5 depicts, the proposed simplified decoder achieves about 1 dB gain over the sphere decoder at BER = 10^{-4}.

Figure 6 shows the simulation results for 4 transmit antennas, a channel with 5 µs delay spread, and the system with N = 2048 subcarriers. QPSK and BPSK constellations have been used for the proposed and the BCDD codes to achieve the bit transmission rate of 1 bit/s/Hz. Suboptimum sphere decoders are used for both codes; also the simplified decoder is utilized for our proposed code. As BER values in Fig. 6 show, our proposed code outperforms that of the BCDD when the sphere decoder is used and it approximately leads to the same performance as the BCDD code when the simplified decoder is used.

In Fig. 7, we simulated our proposed scheme and BCDD code for different channel models. We have considered two channels, one 2-ray channel with 15 µs delay spread and equal power and one 4-ray channel with $\boldsymbol{\zeta} = [0, 6.5, 7.7, 15]$ and $\delta^2 = [0.42, 0.26, 0.18, 0.14]$. As simulation results show, by increasing the number of channel taps L, the performance of codes improves.

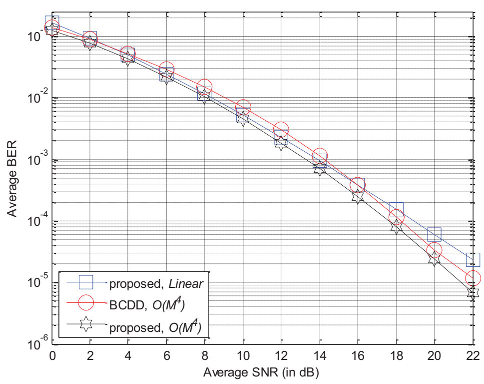

Fig. 4. BER performance for the 2-ray equal power frequency-selective channel with 5 µs delay spread, BPSK constellation, N = 1024, K = 1, M_t=2, M_r=1, γ_{SD}= γ_{dpi} = 16, 1 bit/s/Hz.

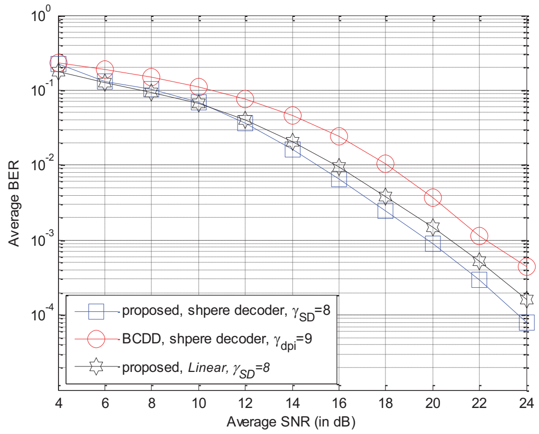

Fig. 5. BER performance for the 2-ray equal power frequency-selective channel with 5 µs delay spread, BPSK constellation, N = 1024, K = 1, M_t = 3, M_r = 1, 3 bits/s/Hz.

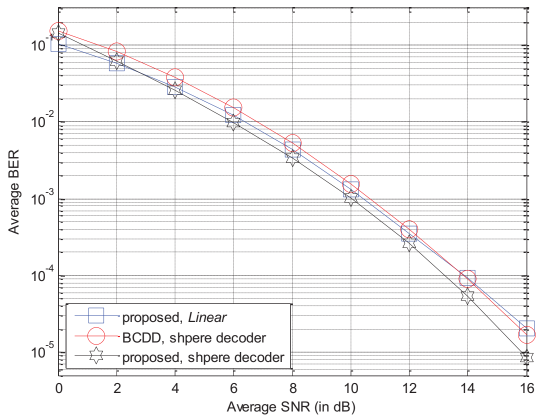

Fig. 6. BER performance for the 2-ray equal power frequency-selective channel with 5 µs delay spread, N = 2048, K = 1, M_t = 4, M_r = 1, γ_{SD} = γ_{dpi} = 16, 1 bit/s/Hz.

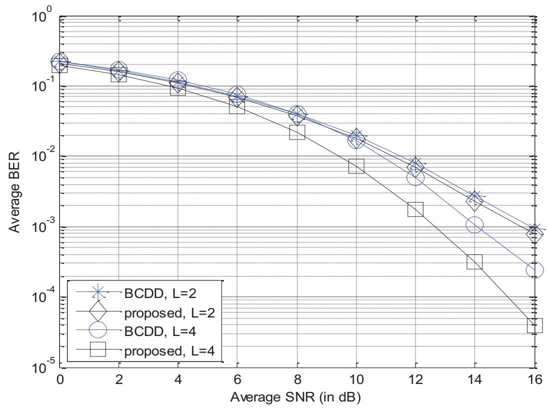

Fig. 7. BER performance for two frequency-selective channels with L = 2 ($\boldsymbol{\zeta} = [0, 15]$ and $\delta^2 = [0.5, 0.5]$) and L=4 ($\boldsymbol{\zeta} = [0, 6.5, 7.7, 15]$ and $\delta^2 = [0.42, 0.26, 0.18, 0.14]$), QPSK constellation, N = 64, K = 1, M_t = 2, M_r = 1, γ_{SD} = γ_{dpi} = 16, 1 bit/s/Hz.

6. Conclusion

In this paper we designed a new class of full-diversity space-time-frequency block codes with high coding advantage over a fast frequency selective fading channel when channel side information is available at the transmitter side or not. Using simulation results, we verified that our proposed codes outperform one of the best proposed codes in the literature. For our proposed codes the ML decoder has a complexity in the order of $\mathcal{O}(M^{KLM_t})$, so the decoding complexity increases exponentially with increasing the number of transmit antennas, channel taps and OFDM blocks. For our codes, we introduced an alternative decoding method with *linear complexity* which performs properly for codes designed for an arbitrary number of transmit antennas and 2-ray frequency-selective channels. The proposed scheme degrees the performance of proposed STFBCs, but due to the significant reduction in the complexity of the receiver could still be of interest. The simplified decoder performs satisfactorily for the space-frequency block codes version of our proposed coding scheme rather than the proposed STFBCs.

7. Appendix

In this appendix, we prove that the designed STF code in (9) in a frequency selective channel with L channel taps can achieve diversity order of $4L$ for 2 transmit antennas and the real constellations.

Proof: According to the proof of full diversity in Appendix I in [19], our proposed code is full diversity if $\prod_{k=1}^{K}\det(\boldsymbol{\Gamma}_k) \neq 0$ for $x_\mathrm{i} \neq x'_\mathrm{i}$. Now, for $K = 2$, we have:

$$\boldsymbol{\Gamma_1} \triangleq \boldsymbol{D_1} \circ \boldsymbol{T} \in \mathbb{C}^{2L\times 2L} \tag{30}$$

where

$$\mathbf{D_1} = \begin{bmatrix} \sigma_0\Delta_1 & \sigma_0\Delta_2 & \cdots & \sigma_{L-1}\Delta_1 & \sigma_{L-1}\Delta_2 \\ \sigma_0\Delta_2^* & \sigma_0\Delta_1^* & \cdots & \sigma_{L-1}\Delta_2^* & \sigma_{L-1}\Delta_1^* \\ \sigma_0\Delta_3 & \sigma_0\Delta_4 & \cdots & \sigma_{L-1}\Delta_3 & \sigma_{L-1}\Delta_4 \\ \sigma_0\Delta_4^* & \sigma_0\Delta_3^* & \cdots & \sigma_{L-1}\Delta_4^* & \sigma_{L-1}\Delta_3^* \\ \vdots & \vdots & \cdots & \vdots & \vdots \\ \sigma_0\Delta_{2L-1} & \sigma_0\Delta_{2L} & \cdots & \sigma_{L-1}\Delta_{2L-1} & \sigma_{L-1}\Delta_{2L} \\ \sigma_0\Delta_{2L}^* & \sigma_0\Delta_{2L-1}^* & \cdots & \sigma_{L-1}\Delta_{2L}^* & \sigma_{L-1}\Delta_{2L-1}^* \end{bmatrix} \in \mathbb{C}^{2L\times 2L} \tag{31}$$

and

$$\boldsymbol{\Gamma_2} \triangleq \boldsymbol{D_2} \circ \boldsymbol{T} \in \mathbb{C}^{2L\times 2L} \tag{32}$$

where

$$\mathbf{D_2} = \begin{bmatrix} \sigma_0\Delta_{2L+1} & \sigma_0\Delta_{2L+2} & \cdots & \sigma_{L-1}\Delta_{2L+1} & \sigma_{L-1}\Delta_{2L+2} \\ \sigma_0\Delta_{2L+2}^* & \sigma_0\Delta_{2L+1}^* & \cdots & \sigma_{L-1}\Delta_{2L+2}^* & \sigma_{L-1}\Delta_{2L+1}^* \\ \sigma_0\Delta_{2L+3} & \sigma_0\Delta_{2L+4} & \cdots & \sigma_{L-1}\Delta_{2L+3} & \sigma_{L-1}\Delta_{2L+4} \\ \sigma_0\Delta_{2L+4}^* & \sigma_0\Delta_{2L+3}^* & \cdots & \sigma_{L-1}\Delta_{2L+4}^* & \sigma_{L-1}\Delta_{2L+3}^* \\ \vdots & \vdots & \cdots & \vdots & \vdots \\ \sigma_0\Delta_{4L-1} & \sigma_0\Delta_{4L} & \cdots & \sigma_{L-1}\Delta_{4L-1} & \sigma_{L-1}\Delta_{4L} \\ \sigma_0\Delta_{4L}^* & \sigma_0\Delta_{4L-1}^* & \cdots & \sigma_{L-1}\Delta_{4L}^* & \sigma_{L-1}\Delta_{4L-1}^* \end{bmatrix} \in \mathbb{C}^{2L\times 2L}. \tag{33}$$

In above equations, $\Delta_\mathrm{i} = x_\mathrm{i} - x'_\mathrm{i}$, where x_i's and x'_i's are symbols associated to 2 distinct codewords $\boldsymbol{C}$ and $\widehat{\boldsymbol{C}}$, and $\mathbf{T} \in \mathbb{C}^{2L\times 2L}$ is as follows:

$$\mathbf{T} = \begin{bmatrix} 1 & 1 & \cdots & 1 & 1 \\ -w^{\zeta_0} & w^{\zeta_0} & \cdots & -w^{\zeta_{L-1}} & w^{\zeta_{L-1}} \\ w^{2\zeta_0} & w^{2\zeta_0} & \cdots & w^{2\zeta_{L-1}} & w^{2\zeta_{L-1}} \\ -w^{3\zeta_0} & w^{3\zeta_0} & \cdots & -w^{3\zeta_{L-1}} & w^{3\zeta_{L-1}} \\ \vdots & \vdots & \cdots & \vdots & \vdots \\ -w^{(2L-1)\zeta_0} & w^{(2L-1)\zeta_0} & \cdots & -w^{(2L-1)\zeta_{L-1}} & -w^{(2L-1)\zeta_{L-1}} \end{bmatrix}. \tag{34}$$

Therefore, $\mathbf{T}$ could be rewritten as follows:

$$\mathbf{T} = \boldsymbol{V}\left(-w^{\zeta_0}, w^{\zeta_0}, -w^{\zeta_1}, w^{\zeta_1}, \ldots, -w^{\zeta_{L-1}}, w^{\zeta_{L-1}}\right) \in \mathbb{C}^{2L\times 2L}. \tag{35}$$

It is obtained numerically that the minimum value of $\prod_{k=1}^{K}\det(\boldsymbol{\Gamma}_k)$ is achieved when all s_i's and s'_i's are the same except for s_1 and s'_1 , i.e., $\Delta_1 \neq 0$. So, we have:

$$\widehat{\boldsymbol{\Gamma}}_\mathbf{1} \triangleq \widehat{\mathbf{D}}_\mathbf{1} \circ \mathbf{T} \in \mathbb{C}^{2L\times 2L}, \tag{36}$$

$$\widehat{\boldsymbol{\Gamma}}_\mathbf{2} \triangleq \widehat{\mathbf{D}}_\mathbf{2} \circ \mathbf{T} \in \mathbb{C}^{2L\times 2L} \tag{37}$$

where

$$\widehat{\mathbf{D}}_\mathbf{1} = \widehat{\mathbf{D}}_\mathbf{2} = \begin{bmatrix} \sigma_0\Delta_1 & \sigma_0\Delta_1 & \cdots & \sigma_{L-1}\Delta_1 & \sigma_{L-1}\Delta_1 \\ \sigma_0\Delta_1^* & \sigma_0\Delta_1^* & \cdots & \sigma_{L-1}\Delta_1^* & \sigma_{L-1}\Delta_1^* \\ \sigma_0\Delta_1 & \sigma_0\Delta_1 & \cdots & \sigma_{L-1}\Delta_1 & \sigma_{L-1}\Delta_1 \\ \sigma_0\Delta_1^* & \sigma_0\Delta_1^* & \cdots & \sigma_{L-1}\Delta_1^* & \sigma_{L-1}\Delta_1^* \\ \vdots & \vdots & \cdots & \vdots & \vdots \\ \sigma_0\Delta_1 & \sigma_0\Delta_1 & \cdots & \sigma_{L-1}\Delta_1 & \sigma_{L-1}\Delta_1 \\ \sigma_0\Delta_1^* & \sigma_0\Delta_1^* & \cdots & \sigma_{L-1}\Delta_1^* & \sigma_{L-1}\Delta_1^* \end{bmatrix} \in \mathbb{C}^{2L\times 2L}. \tag{38}$$

So, determinant of $\widehat{\boldsymbol{\Gamma}}$ is equal to:

$$\det(\widehat{\boldsymbol{\Gamma}}_\mathbf{2}) = \det(\widehat{\boldsymbol{\Gamma}}_\mathbf{1}) = \prod_{i=0}^{L-1}\sigma_i^2 \times |\Delta_1|^{2L} \times \det(\mathbf{T}). \tag{39}$$

Therefore,

$$\prod_{k=1}^{2}\det(\boldsymbol{\Gamma}_k) = \left(\prod_{i=0}^{L-1}\sigma_i^2 \times |\Delta_1|^{2L} \times \det(\mathbf{T})\right)^2. \tag{40}$$

In (39), $\det(\mathbf{T})$ is non-zero, because $\mathbf{T}$ is a Vandermonde matrix as follows:

$$\mathbf{T} = \boldsymbol{V}\left(-w^{\zeta_0}, w^{\zeta_0}, -w^{\zeta_1}, w^{\zeta_1}, \ldots, -w^{\zeta_{L-1}}, w^{\zeta_{L-1}}\right) \in \mathbb{C}^{2L\times 2L} \tag{41}$$

and

$$\det(\boldsymbol{V}(t_1, t_2, \ldots, t_n)) = \prod_{\substack{\mu,\nu=1 \\ \mu>\nu}}^{n}(t_\mu - t_\nu) \tag{42}$$

and because $\zeta_0 < \cdots < \zeta_{L-2} < \zeta_{L-1}$, $\det(\mathbf{T})$ and then $\prod_{k=1}^{K}\det(\boldsymbol{\Gamma}_k)$ are non-zero. So the rank of $\widehat{\boldsymbol{\Gamma}}_1$ and $\widehat{\boldsymbol{\Gamma}}_2$ is $2L$ and thus the diversity advantage of the proposed code when we consider 2 OFDM symbols in a fast frequency selective channel is equal to $4LM_r$.

References

[1] ALAMOUTI, S. A simple transmit diversity technique for wireless communications. *IEEE Journal on Selected Areas in Communications*, 1998, vol. 16, no. 8, p. 1451 - 1458.

[2] TAROKH, V., JAFARKHANI, H., CALDERBANK, A. R. Space-time block codes from orthogonal design. *IEEE Transactions on Information Theory*, 1999, vol. 45, no. 5, p 1456 - 1467.

[3] BIDAKI, S. S. H., TALEBI, S., SHAHABINEJAD, M. A full-rate full-diversity 2×2 space-time block code with linear complexity for the maximum likelihood receiver. *IEEE Communications Letters*, 2011, vol. 15, no. 8, p. 842 - 844.

[4] SEZGINER, S., SARI, H., BIGLIERI, E. On high-rate full-diversity 2×2 space-time codes with low-complexity optimum detection. *IEEE Transactions on Communications*, 2009, vol. 57, no. 5, p. 1532 - 1541.

[5] LIU, J., ZHANG, J.-K., WONG, K. M. Full-diversity codes for MISO systems equipped with linear or ML detectors. *IEEE Transactions on Information Theory*, 2008, vol. 54, no. 10, p. 4511 -4527.

[6] FOZUNBAL, M., MCLAUGHLIN, S. W., SCHAFER, R. W. On space-time-frequency coding over MIMO-OFDM systems. *IEEE Transactions on Wireless Communications*, 2005, vol. 4, no. 1, p. 320 - 331.

[7] AGRAWAL, D., TAROKH, V., NAGUIB, A., SESHADRI, N. Space-time coded OFDM for high data-rate wireless communication over wideband channels. In *Proceedings IEEE VTC Spring* '98. 1998, p. 2232 - 2236.

[8] SHAO, L., ROY, S. Rate-one space-frequency block codes with maximum diversity for MIMO-OFDM. *IEEE Transactions on Wireless Communications*, 2005, vol. 4, no. 4, p. 1674 - 1687.

[9] ZHANG, W., XIA, X.-G., CHING, P. C., WANG, H. Rate two full diversity space-frequency code design for MIMO-OFDM. In *Proceedings of IEEE SPAWC*. New York (NY, USA), 2005, p. 303 - 307.

[10] MOHAMMADIAN, Z., SHAHABINEJAD, M., TALEBI, S. New full-diversity space-frequency block codes based on the OSTBCs. *IEEE Communications Letters*, 2012, vol. 16, no. 8, p. 1620 - 1623.

[11] ZHANG, W., XIA, X.-G., LETAIEF, K. B. Space-time/frequency coding for MIMO-OFDM in next generation broadband wireless systems. *IEEE Wireless Communications Magazine*, 2007, vol. 14, no. 3, p. 32 - 43.

[12] SU, W., SAFAR, Z., LIU, K. J. R. Towards maximum achievable diversity in space, time and frequency: Performance analysis and code design. *IEEE Transactions on Wireless Communications*, 2005, vol. 4, no. 4, p. 1847 - 1857.

[13] VENTURINO, L., PRASAD, N., WANG, X., MADIHIAN, M. Design of linear dispersion codes for practical MIMO-OFDM systems. *IEEE Journal of Selected Topics in Signal Processing*, 2007, vol. 1, no. 1, p. 178 - 188.

[14] SHANKAR, M. R. B., HARI, K. V. S. Systematic construction of linear transform based full-diversity, rate-one space–time frequency codes. *IEEE Transactions on Signal Processing*, 2009, vol. 57, no. 6, p. 2285 - 2298.

[15] FAZEL, F., JAFARKHANI, H. Quasi-orthogonal space-frequency and space-time-frequency block codes for MIMO OFDM channels. *IEEE Transactions on Wireless Communications*, 2008, vol. 7, p. 184 - 192.

[16] SHAHABINEJAD, M., TALEBI, S. Full-diversity space-time-frequency coding with very low complexity for the ML decoder. *IEEE Communications Letters*, 2012, vol. 16, no. 5, p. 658 - 661.

[17] LEE, K., KIM, Y., KANG, J. A novel orthogonal space-time-frequency block code for OFDM systems. *IEEE Communications Letters*, vol. 13, no. 9, p. 652 - 654.

[18] MA, X., GIANNAKIS, G. B. Space-time-multipath coding using digital phase sweeping or circular delay diversity. *IEEE Transactions on Signal Processing*, 2005, vol. 53, no. 3, p. 1121 - 1131.

[19] ZHANG, W., XIA, X.-G., CHING, P. C. High-rate full-diversity space time-frequency codes for broadband MIMO block-fading channels. *IEEE Transactions on Communications*, 2007, vol. 55, p. 25 - 34.

About Authors ...

Mostafa SHAHABINEJAD received his B.Sc. and M.Sc. degrees in Electrical Engineering-Telecommunications from Shahid Bahonar University of Kerman, Kerman, Iran, in 2009 and 2011, respectively. His research interests include coding techniques in Networks, MIMO and MIMO–OFDM systems.

Zahra MOHAMMADIAN received her B.S. degree in Communication Engineering from Sistan and Baluchestan University of Zahedan, Iran in 2010 and her M.S. degree from Shahid Bahonar University of Kerman, Kerman, Iran in 2012. She is currently a Ph.D. student in the Shiraz University of Technology, Shiraz, Iran. Her research interests are in the field of multiple-input multiple-output orthogonal frequency-division multiplexing (MIMO-OFDM) systems and space-time coding.

Siamak TALEBI received B.S. and M.S. degrees in Communication Engineering, from Isfahan University of Technology, in 1989 and 1992 respectively and a Ph.D. degree from the University of London (King's College), in 2001. He is currently with the Department of Electrical Engineering at Shahid Bahonar University of Kerman, in Iran and the Advanced Communications Research Institute at Sharif University of Technology, Tehran, Iran. His research interests include wireless communications, cognitive radio, MIMO–OFDM and also video coding.